International Journal of Biological Macromolecules 321 (2025) 146349

Contents lists available at ScienceDirect

International Journal of Biological Macromolecules

journal homepage: www.elsevier.com/locate/ijbiomac

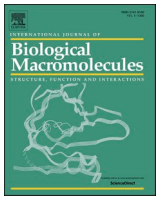

Coordinated dysfunction in oxidative phosphorylation–related proteins and a delayed acrosome reaction during sperm capacitation reduces male fertility

Yoo-Jin Park, Gangaraju Gedda, Myung-Geol Pang *

Department of Animal Science & Technology and BET Research Institute, Chung-Ang University, Anseong, Gyeonggi-do 17546, Republic of Korea

ARTICLE INFO

Keywords:
Sperm capacitation
Fertility
Oxidative phosphorylation

ABSTRACT

Although dynamic changes of proteomes during sperm capacitation are well documented by the advanced proteomic research, spatiotemporal changed proteins during capacitation according to sperm fertility remain elusive. This study aimed to investigate temporal protein changes in spermatozoa during capacitation in relation to fertility status. Initially, proteomic analysis was conducted on spermatozoa at early (20 min) and late (120 min) stages of capacitation to comprehensively identify protein modifications during capacitation, irrespective of fertility status (n = 6). After late capacitation, a decrease in acrosome vesicle-associated proteins and an increase in oxidative phosphorylation (OXPHOS)-related proteins were observed. To determine whether these temporal protein changes are linked to fertility status, western blot were conducted using normal fertility (NF, n = 5) and below-normal fertility (BNF, n = 5) bulls during capacitation. We found that mitochondrial respiratory complex proteins II–IV were abundant in BNF spermatozoa before and during capacitation. During capacitation, NF sperm showed gradual acrosomal protein degradation, while BNF sperm retained intact proteins and showed higher ROS accumulation in the acrosome after late capacitation. These results suggest that systemic instability in OXPHOS may promote ROS accumulation in the acrosome during late capacitation, potentially delaying the acrosome reaction and thereby reducing fertility.

1. Introduction

According to a 2024 World Health Organization report, over 15 % of reproductive-aged couples experience infertility, which is rapidly emerging as a global public health issue [1,2]. Infertility can lead to higher social/individual burdens in terms of diagnosis and treatment, as well as emotional and psychological distress [2,3]. Although infertility is primarily caused by abnormal physiological conditions or underlying diseases, the cause of 15 % of infertility remains unclear [4]. Idiopathic infertility refers to unsuccessful conception despite the absence of identifiable causes, such as hormonal imbalances, morphological abnormalities in the reproductive tract, or defects in sperm and oocytes. Because idiopathic infertility cannot be assessed clearly using clinical methods, overtreatment or irrelevant treatment are often prescribed to infertile couples, leading to unnecessary fertility care costs [5,6]. Moreover, the potential risks associated with assisted reproduction technologies can inevitably increase cancer risk and psychological and health stress in children [7]. Similarly, unsuccessful artificial insemination in the animal industry causes major economic losses because of reduced offspring productivity [8–10]. Because male infertility accounts for approximately 50 % of all infertility cases, semen quality assessment is usually performed before artificial insemination or clinical trials [9,11]. However, commercial semen analysis (e.g., assessing parameters such as sperm motility, morphology, and membrane integrity) has shown little predictive value for assessing male fertility [12,13]. Therefore, advanced diagnostic methods should be developed by deciphering the underlying mechanisms of male infertility.

Sequential and multifactorial processes are required to establish the fertilising ability of spermatozoa, from development in the testes (spermatogenesis) to functional maturation in the female reproductive tract (capacitation and acrosome reaction) [14–17]. Following testicular development, spermatozoal proteins undergo post-translational modifications that facilitate the remodelling or modification of intrinsic protein and lipid structures in the epididymis [18,19]. As a consequence of maturation, mature spermatozoa undergo molecular changes and

* Corresponding author at: 4726 Seodong-daero, Deadeok-myon, Anseong, Gyeonggi-do 17546, Republic of Korea.
E-mail address: mgpang@cau.ac.kr (M.-G. Pang).

https://doi.org/10.1016/j.ijbiomac.2025.146349
Received 15 May 2025; Received in revised form 24 July 2025; Accepted 25 July 2025
Available online 30 July 2025

membrane-surface remodelling (referred to as capacitation) to acquire fertilising ability while moving through the female reproductive tract [20]. Previous report showed that various proteins involved in regulating oxidative stress, motility acquisition, capacitation, and the acrosome reaction undergo dynamically changes during capacitation, which regulates sperm fertility [9,21–23]. Since phosphorylation was discovered in spermatozoa, the prevailing view has been that biochemical and physiological changes during sperm capacitation are driven by post-translational modifications, as spermatozoa are transcriptionally and translationally inactive [18,19]. However, we recently showed that protein modifications during sperm capacitation occur concomitantly with translation in spermatozoa [16]. Importantly, acrosome reaction-associated proteins changed dynamically during the initial capacitation stage, indicating that spermatozoa undergo preparations for the next step of the acrosome reaction [16]. Regarding various proteins that are sequentially modified to maintain functionality and fertility, a comprehensive analysis of time-dependent protein modification during sperm capacitation is required to understand the complex physiological and biochemical mechanisms of male fertility. Therefore, in this study, we explored time-dependent protein dynamics during sperm capacitation using liquid chromatography–tandem mass spectrometry (LC-MS/MS) to screen for comprehensive protein modifications during sperm capacitation and the acrosome reaction. To best reflect the dynamic changes in the sperm proteome that occur under in vivo capacitation conditions, we applied an experimental protocol using 10 μg/mL heparin for 20 min incubation—our previously optimized capacitation condition—which closely resembles the physiological environment and supports accurate assessment of sperm fertility [24]. Our proteomic analysis revealed that acrosomal vesicle proteins were upregulated during early capacitation, whereas proteins related to oxidative phosphorylation (OXPHOS) were predominantly increased during the late capacitation phase. Given that reactive oxygen species (ROS) are generated as byproducts of OXPHOS and play dual roles as both signaling molecules and stressors in spermatozoa depending on their intracellular levels [14,25], we further examined how intracellular ROS accumulation during capacitation correlates with male fertility status.

2. Materials and methods

2.1. Sperm source and fertility records

All animal experiments were approved by the Institutional Animal Care and Use Committee (IACUC) of Chung-Ang University, Seoul, Korea (IACUC approval number: 2016–00009). We used bovine spermatozoa to model male fertility because previous data showed that the semen samples were homogenous and exhibited a broad range of fertility [26]. Frozen bovine semen samples from Hanwoo cattle (native to Korea) with at least 50 insemination records were purchased from the Hanwoo Improvement Program of the National Agriculture Cooperative Federation of Korea. Fertility rate was defined as the ratio of the total number of pregnant cows (which did not show oestrus gain) to the total number of inseminated cows, according to our previous study. Semen samples were divided into normal fertility (NF; 77.44 ± 1.51, n = 5) and below-normal fertility (BNF; 60.51 ± 1.61, n = 5) groups. Each individual semen sample serving as both a biological and technical replicate.

2.2. Sperm preparation for capacitation triggering

To establish sperm capacitation conditions similar to that in the female reproductive tract, 10 μg/mL heparin was added to Tyrode albumin lactated pyruvate medium (capacitation medium, CM) containing 100 mM NaCl, 3.1 mM KCl, 2.0 mM $CaCl{\bullet}2H_2O$, 0.4 mM $MgCl{\bullet}6H_2O$, 0.3 mM $Na_2HPO_4{\bullet}12H_2O$, 21.6 mM sodium lactate, 25 mM $NaHCO_3$, 1.0 mM sodium pyruvate, 0.6 % bovine serum albumin, which was optimal in our previous study [24]. Percoll-separated motile spermatozoa were incubated in CM for 20 min (early capacitation) or 120 min (late capacitation) to induce capacitation and acrosome reactions, respectively [16]. The capacitation status was analysed via chlortetracycline/Hoechst staining (CTC/H33258 staining), as previously described [28].

2.3. LC-MS/MS analysis

To explore the comprehensive proteome changes during sperm capacitation regardless fertility, six individual semen samples (three randomly selected from each fertility group) were used. LC-MS/MS analysis of spermatozoa was performed at the Korea Basic Science Institute (Ochang Headquarters, Division of Bioconvergence Analysis), as described previously [16]. Functionally capacitated (CP) and acrosome-reacted (AR) spermatozoa were lysed for 1 h in sample buffer consisting of 65.8 mM Tris-HCl, 1 % sodium dodecyl sulphate (SDS), 10 % glycerol, 0.05 % bromophenol blue, and 5 % β-mercaptoethanol. The sperm cell lysates were resolved by 12 % SDS-polyacrylamide gel electrophoresis, visualised via Coomassie Brilliant Blue staining, and excised for LC-MS/MS. Tryptic digestion was performed in 50 mM ammonium bicarbonate at 37 °C for 12–16 h. Tryptic peptides was extracted with an extraction solution (50 mM ammonium bicarbonate and 50 % acetonitrile containing 5 % trifluoroacetyl acid [TFA]). Lyophilised peptides resuspended in 0.5 % TFA were first loaded onto a 100 μm × 2 cm nanoviper trap column, then separated on a 15 cm × 75 μm nanoviper analysis column (Thermo Fisher Scientific) at a flow rate of 300 nL/min, and eluted with a gradient of 5 % – 40 % acetonitrile over 95 min. All MS and MS/MS spectra captured using a Q Exactive Plus mass spectrometer (Thermo Fisher Scientific) were acquired in the data-dependent top 12 mode. The MS/MS data were analysed using MASCOT 2.7 software, with a false-discovery rate (FDR) set to <1 %.

2.4. Proteomic data and signaling-pathway analyses

Quantitative proteomic data analysis was performed using the Perseus software platform (version 2.1.3.0) according to previous studies [29,30], with some modifications. Briefly, a heatmap was generated to visualise significant differences in protein expression between non-capacitated (NCP), CP, and AR spermatozoa. Hawaii plots displayed protein expression differences between NCP and CP or AR spermatozoa. Protein interactions and Gene Ontology (GO) terms enriched among differentially expressed proteins during sperm capacitation and the acrosome reaction were visualised using the STRING application (version 2.0.0) in Cytoscape software (version 3.10.3).

2.5. Western blot analysis

To determine whether proteins that were differentially expressed during capacitation varied with sperm fertility, we compared protein expression levels between NF and BNF spermatozoa (n = 5 for each group) at different capacitation stages via western blot analysis. Cell lysates of NCP, CP, and AR spermatozoa from the NF and BNF groups were loaded onto 4–12 % Mini-PROTEAN TGX Precast Protein Gels (Bio-Rad). Next, the proteins were transferred to 0.2 μm Hybond LFP polyvinylidene difluoride membranes (Amersham). The membranes were blocked for 1 h with 5 % skim milk in phosphate buffered saline (PBS) with 1 % Tween-20 (PBS-T) and then incubated with an anti- NADH: ubiquinone oxidoreductase core subunit S8 (NDUFS8), anti-ATP synthase F (0) complex subunit B1, mitochondrial (ATP5F1), anti-GLUT3, anti-Total OXPHOS Rodent WB Antibody Cocktail and an anti-α-tubulin antibody. To detect protein tyrosine phosphorylation in spermatozoa, membranes were blocked with 3 % bovine serum albumin (BSA) and incubated with an anti-phosphotyrosine antibody (P-Tyr-100).

Following overnight incubation with primary antibodies at 4 °C, the membranes were washed with PBS-T and incubated with horseradish peroxidase-conjugated secondary antibodies for 2 h at room

temperature. Clarity ECL Western Blotting Substrate (Bio-Rad)-treated membranes were loaded onto an eBLOT system (eBlot Photoelectric Technology) to assess the protein expression levels.

2.6. Immunofluorescence staining of spermatozoa

To assess changes in protein expression and localisation during sperm capacitation, immunofluorescence staining was performed as we described previously [21], with some modifications. Briefly, the spermatozoa were dried on slides and fixed in 4 % paraformaldehyde (Sigma-Aldrich) for 30 min at room temperature. The washed slides were blocked with PBS-T containing 3 % BSA for 30 min at room temperature and incubated overnight with antibodies against glutathione peroxidase 4 (GPX4; LSBIO), actin-related protein T2 (ACTRT2; Abcam), glucose transporter 3 (GLUT3; Abcam), and acrosomal vesicles (Invitrogen). Subsequently, the slides were washed with PBS and stained with secondary antibodies conjugated to Alexa 488 (Invitrogen) or Alexa 568 (Invitrogen). Moreover, to investigate the differences in intracellular ROS production in spermatozoa after 2 h of capacitation, intracellular ROS levels were visualised using CellROX Green® Oxidative Stress Reagents (Invitrogen), following the manufacturer's instructions. Lectin peanut agglutinin (PNA) conjugated with Alexa 598 (Invitrogen) was used to stain the acrosomes. Spermatozoa were counterstained using VECTASHIELD (Vector Laboratories), and images were acquired using a LSM 800 confocal microscope (Carl Zeiss). At least three separate semen samples per group were examined, and 400 spermatozoa were assessed in each replicate.

2.7. Statistical analysis

Proteomic data from NCP, CP, and AR spermatozoa were compared using one-way analysis of variance (ANOVA) with MaxQuant and Perseus software (version 2.1.3.0). Changes in the capacitation status and protein expression differences during sperm capacitation between the NF and BNF groups were analysed via two-way ANOVA with GraphPad Prism software (version 10.1.1). Šídák's multiple comparisons test was used to compare differences between NF and BNF at each capacitation time point, while Tukey's multiple comparisons test was applied to assess time-dependent changes in protein expression within each fertility group. Differences in acrosomal protein expression levels between the NF and BNF groups during sperm capacitation were analysed using the chi-square test with GraphPad Prism (version 10 1.1).

3. Results

3.1. Changes in sperm motility, capacitation status, and tyrosine phosphorylation during sperm capacitation

A preliminary study was conducted to evaluate heparin-induced capacitation at multiple time points (0, 20, 30, 60, 120, and 240 min). A significant increase in the proportion of capacitated spermatozoa was observed after 20 min of incubation, while the highest proportion of acrosome-reacted spermatozoa was detected at 120 min (Supplementary Fig. 1A–B, $p < 0.05$). In contrast, the percentage of non-capacitated spermatozoa gradually decreased following incubation compared to 0 min (Supplementary Fig. 1E, $p < 0.05$). Tyrosine phosphorylation levels also decreased after 20 min but remained higher than at 0 min (Supplementary Fig. 1E and G). Notably, 4 h of incubation resulted in >50 % sperm death and motility dropping below 25 % (Supplementary Fig. 1F, $p < 0.05$). While the percentage of motile spermatozoa significantly decreased after 120 min compared to 0 and 20 min, regardless of fertility status, sperm linearity (LIN) and sperm velocity parameters—including average path velocity (VAP) and straight-line velocity (VSL)—were increased at 120 min of capacitation compared to 0 and 20 min (Table 1). Based on these findings, we selected 20 min as the early capacitation stage and 120 min as the late stage, as these time points effectively represent key phases of capacitation without substantially compromising sperm viability or motility.

CTC/H33258 staining was performed to distinguish the capacitation status of spermatozoa, including NCP, CP, and AR spermatozoa (Fig. 1A), as described previously [31]. Significantly more CP spermatozoa were observed during early capacitation than at 0 min ($p < 0.01$), whereas significantly less NCP spermatozoa were observed during early capacitation ($p < 0.001$, Fig. 1B). The number of AR spermatozoa gradually increased with capacitation time ($p < 0.05$, Fig. 1B). Although tyrosine-phosphorylated proteins were slightly less abundant at late capacitation than at early capacitation, they were present at higher levels during capacitation than at 0 min (Fig. 1C).

3.2. Identification of capacitation-related proteins during early and late capacitation

We comprehensively explored time-dependent proteomic changes in spermatozoa during capacitation, regardless of the sperm fertility status. Among 43 proteins that were differentially expressed in spermatozoa at different capacitation times ($p < 0.05$, Fig. 2A), the expressions of 4 and 38 proteins were significantly changed during early and late capacitation, respectively ($p < 0.05$, Fig. 2B, C). Izumo sperm–egg fusion protein 1 (IZUMO1) expression was significantly upregulated, and the expressions of histone H2A, vesicle-associated membrane protein 3, and tektin 5 were significantly downregulated during early capacitation (Fig. 2B, FDR < 0.05). During late capacitation, the expressions of 13 proteins associated with the GO terms 'acrosomal vesicles', 'secretory granule', and 'abnormal germ cell and sperm morphology' were significantly downregulated (FDR < 0.05, Fig. 2B, C). In addition, the expressions of 25 proteins closely related to 'inner mitochondrial membrane protein disease' and 'oxidative phosphorylation' GO terms were upregulated during late capacitation (FDR < 0.05, Fig. 2D). Differentially expressed proteins at early and late capacitation stages, relative to 0 min, are summarized in Table 2.

3.3. Differentially expressed capacitation-related proteins according to fertility status

Considering the important roles of protein dynamics during sperm capacitation in sperm fertility [9,16], we explored whether capacitation-related proteins were differentially expressed during sperm capacitation, according to the fertility status. Among 25 proteins whose expressions were upregulated in spermatozoa during late capacitation, we compared the expression levels of three OXPHOS-related mitochondrial proteins, including NDUFS8, ATP5F1, and GLUT3, between NF and BNF spermatozoa (Fig. 3A). We also analysed protein expression fluctuations in NF and BNF spermatozoa during early and late capacitation, relative to the corresponding expression levels detected at 0 min. Protein expression upregulation and downregulation during sperm capacitation are indicated by values of >0 and < 0, respectively.

No differences were found in NDUFS8 and ATP5F1 protein expression during capacitation (Fig. 3B, C), whereas GLUT3 protein expression significantly increased during late capacitation, regardless of sperm fertility ($p < 0.05$, Fig. 3D). NDUFS8 protein increased expression in NF spermatozoa at late capacitation ($p < 0.05$, Fig. 3B), whereas no difference was detected in BNF spermatozoa during capacitation (Fig. 3B). Although the overall NDUFS8 protein expression levels were static in BNF spermatozoa during capacitation, we detected significant temporal changes in NDUFS8 protein expression, involving a transition from downregulation during early capacitation to upregulation during late capacitation ($p < 0.05$; Fig. 3B). No differences were found in ATP5F1 protein expression during sperm capacitation, regardless of fertility (Fig. 3C). Sustained upregulation of GLUT3 expression was detected in NF spermatozoa from early capacitation onwards, whereas upregulation of GLUT3 expression was detected in BNF spermatozoa beginning at late capacitation, reflecting in a significant difference between the NF and

Table 1
Comparative analysis of sperm motility and kinematic parameters between normal and below-normal spermatozoa during capacitation.

	Capacitation time	Normal	Below-normal
Motility (%)	0 min	76.77 ± 1.13[a]	78.04 ± 0.80 [A]
	20 min	74.52 ± 2.30 [a]	77.64 ± 1.56 [A]
	120 min	59.96 ± 2.80 [b]	59.52 ± 1.95 [B]
HYP (%)	0 min	2.65 ± 1.04	3.81 ± 1.18
	20 min	0.70 ± 0.47	3.17 ± 1.94
	120 min	0.19 ± 0.19	1.01 ± 0.66
VCL	0 min	130.60 ± 4.09	131.83 ± 3.87
	20 min	122.01 ± 5.53	127.96 ± 5.67
	120 min	138.42 ± 5.93	136.76 ± 6.38
VSL	0 min	79.33 ± 4.63[a]	72.60 ± 2.93 [A]
	20 min	79.33 ± 5.44 [a]	83.62 ± 3.40 [A]
	120 min	108.11 ± 6.43 [b]	103.23 ± 7.03[B]
VAP	0 min	76.94 ± 3.42 [a]	75.93 ± 2.73 [A]
	20 min	77.55 ± 4.80 [a]	81.27 ± 2.97 [A,B]
	120 min	102.79 ± 5.74 [b]	97.11 ± 6.29 [B]
LIN	0 min	60.45 ± 2.03 [a]	57.49 ± 1.69 [A]
	20 min	64.59 ± 2.06 [a]	65.69 ± 1.95 [B]
	120 min	77.76 ± 2.09 [b]	75.08 ± 1.99 [C]

a,b significant differences in motility and motion kinematics during capacitation in NF spermatozoa.
A-C significant differences in motility and motion kinematics during capacitation in BNF spermatozoa.

BNF groups ($p < 0.05$, Fig. 3D).

3.4. Differentially expressed OXPHOS proteins according to fertility status

Next, we investigated temporal expression differences of OXPHOS-related proteins according to the fertility status (Fig. 4A). No changes in ATP5A or NDUFB protein expression were detected during capacitation, regardless of sperm fertility (Fig. 4B, F). Ubiquitin-cytochrome *c* reductase core protein 2 (UQCRC2), cytochrome *c* oxidase subunit I (MTCO1), and succinate dehydrogenase complex iron sulphur subunit B (SDHB), were more abundant in BNF spermatozoa than in NF spermatozoa before capacitation ($p < 0.01$, Fig. 4C–E). UQCRC2 protein expression in BNF spermatozoa was consistently higher than that in NF spermatozoa throughout early capacitation ($p < 0.05$, Fig. 4E). However, UQCRC2 protein expression increased significantly in NF spermatozoa during late capacitation to a level comparable to that in BNF spermatozoa (Fig. 4C). Although MTCO1 protein expression was consistently over 3-fold higher in BNF spermatozoa before capacitation, it increased further during early capacitation, resulting in a greater difference between BNF and NF spermatozoa ($p < 0.05$; Fig. 4D). Although SDHB protein expression was significantly higher in BNF spermatozoa than in NF spermatozoa before capacitation ($p < 0.05$), its expression during early and late capacitation was comparable to that in NF spermatozoa (Fig. 4E).

3.5. Differences in GPX4 protein expression during capacitation

Although OXPHOS activation provides sufficient ATP production for

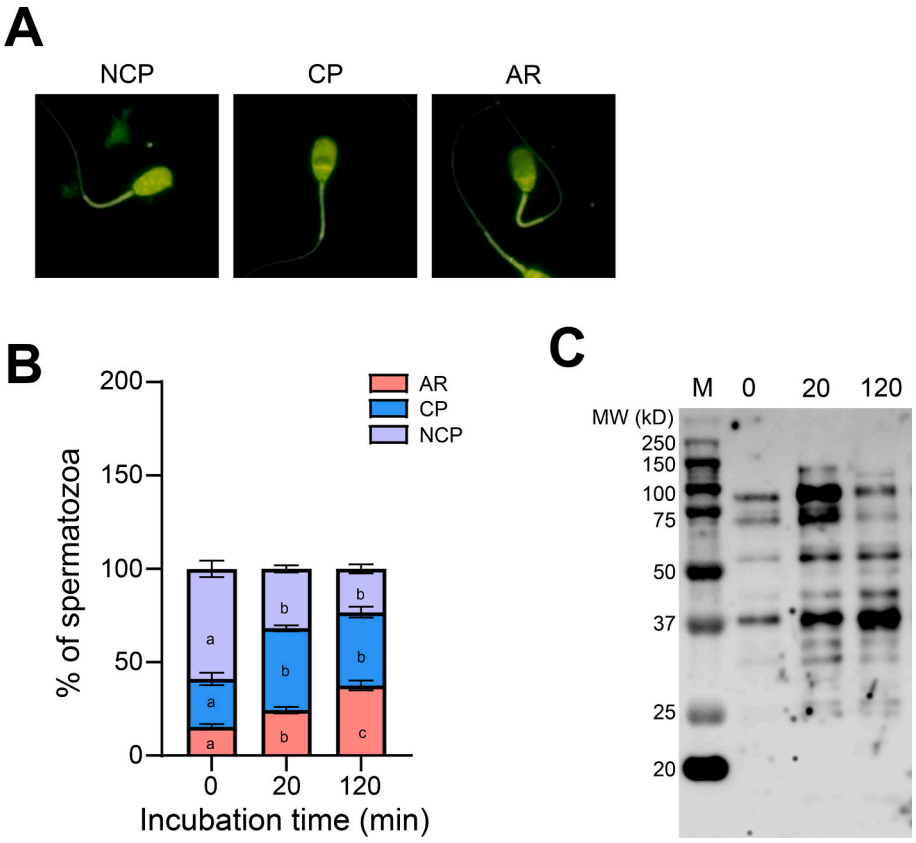

Fig. 1. Changes in the capacitation status and tyrosine phosphorylation during sperm capacitation. (A) Representative chlortetracycline-staining images of live non-capacitated (NCP, bright green fluorescence in entire sperm head), capacitated (CP, bright green fluorescence in the acrosome region), and acrosome-reacted (AR, faint green fluorescence in entire sperm head) spermatozoa. (B) Relative percentages of NCP, CP, and AR spermatozoa during capacitation (0, 20, and 120 min). Values with different superscripts (a, b, c) showed significantly differences between the 0, 20, and 120 min time points for NCP, CP, and AR spermatozoa, as determined by chi-square test. (C) Representative western blot image of phosphor-tyrosine proteins in NF and BNF spermatozoa during capacitation.

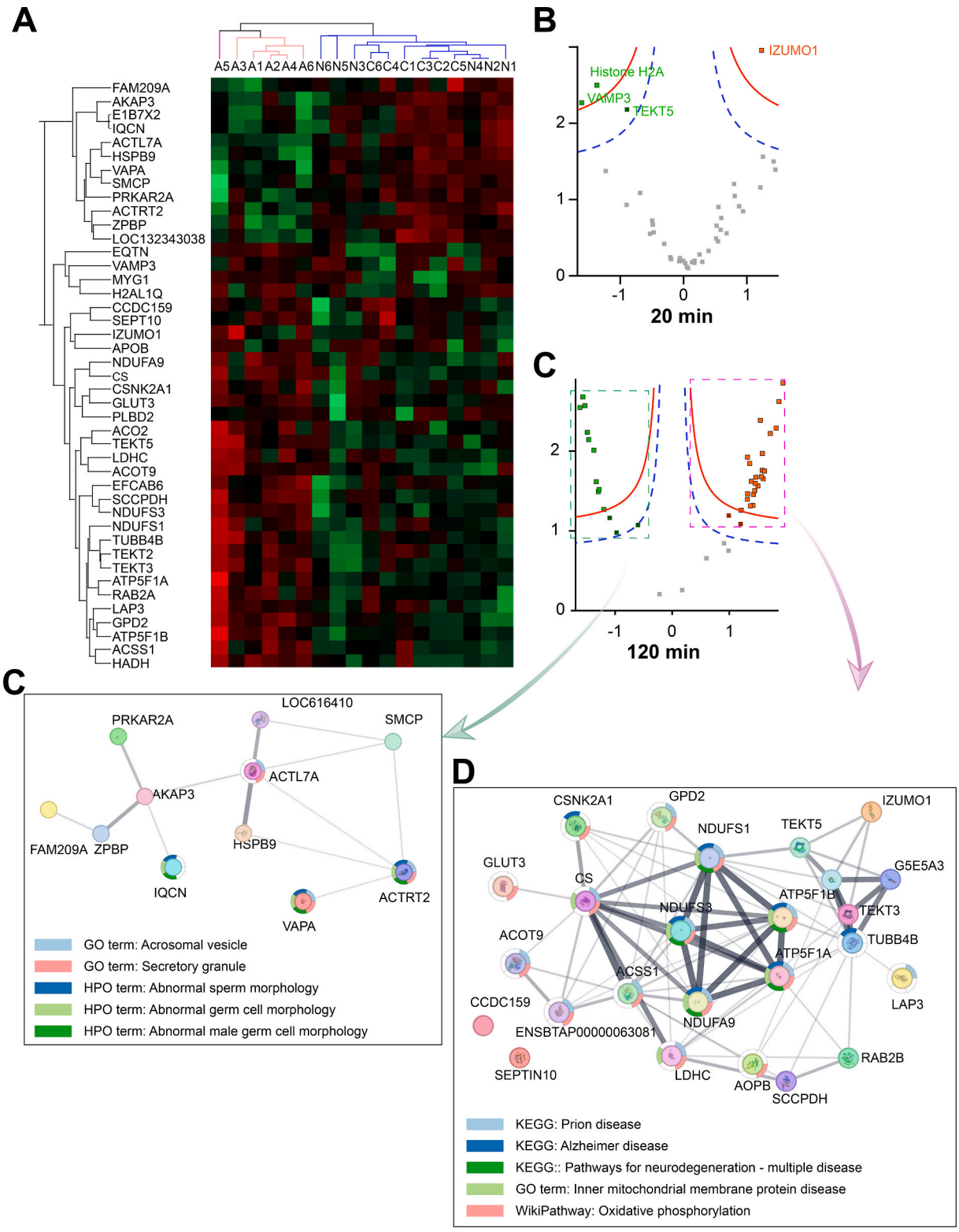

Fig. 2. Changes in the sperm proteome and signaling pathways during capacitation.
(A) Heatmap representing significantly differentially expressed proteins during sperm capacitation. One-way analysis of variance analysis with MaxQuant and Perseus software was performed to compare the non-capacitated (NCP), capacitated (CP), and acrosome-reacted (AR) groups. (B, C) Hawaii plots displayed protein-expression differences between (B) NCP (0 min) and CP (20 min) or (C) NCP (0 min) and AR (120 min) spermatozoa. (D, E) Protein–protein-interaction networks based on the differentially expressed proteins at (D) 20 min or (E) 120 min (relative to the expression levels at 0 min) were analysed and visualised using the STRING application in Cytoscape.

Table 2
Differentially expressed proteins identified by LC-MS/MS during early and late capacitation compared to 0 min.

Capacitation time	Protein name	Uniprot ID	Fold changes	Functional annotation (GO term and KEGG)
Early (20 min)	Izumo sperm-oocyte fusion 1 (IZUMO1)	E1BDA8	1.16	***GOBP*** fusion of sperm to egg plasma membrane involved in single fertilisation; heterotypic cell-cell adhesion; sperm-egg recognition
	Tektin-5 (TEKT5)	Q2YDI7	−0.96	***GOBP*** cilium assembly; cilium movement involved in cell motility; flagellated sperm motility
	Vesicle-associated membrane protein 3 (VAMP3)	Q2KJD2	−1.68	***GOBP*** positive regulation of receptor recycling; protein transport; retrograde transport, endosome to Golgi; SNARE complex assembly; substrate adhesion-dependent cell spreading; vesicle fusion; vesicle-mediated transport ***KEGG*** Phagosome; Salivary secretion; SNARE interactions in vesicular transport; Vasopressin-regulated water reabsorption
	Histone H2A	A0A3Q1LYJ4	−1.44	***GOBP*** heterochromatin formation
Late (120 min)	EF-hand calcium binding domain 6 (EFCAB6)	G5E5A3	1.54	***GOBP*** flagellated sperm motility
	Glucose transporter type 3 (GLUT-3)	P58352	1.52	***GOBP*** D-glucose import; D-glucose transmembrane transport; dehydroascorbic acid transport; galactose transmembrane transport
	NADH dehydrogenase [ubiquinone] iron-sulphur protein 3, mitochondrial (NDUFS3)	P23709	1.50	***GOBP*** mitochondrial electron transport, NADH to ubiquinone; mitochondrial respiratory chain complex I assembly; reactive oxygen species metabolic process ***KEGG*** Alzheimer's disease; Huntington's disease; Oxidative phosphorylation; Parkinson's disease
	L-lactate dehydrogenase (LDHC)	E1BNS9	1.50	***GOBP*** ATP biosynthetic process; flagellated sperm motility; lactate biosynthetic process from pyruvate; lactate metabolic process; pyruvate catabolic process; pyruvate metabolic process
	Casein kinase II subunit alpha (CSNK2A1)	P68399	1.49	***GOBP*** apoptotic process; double-strand break repair; negative regulation of apoptotic signaling pathway; negative regulation of double-strand break repair via homologous recombination; positive regulation of aggrephagy; positive regulation of cell growth; positive regulation of cell population proliferation; positive regulation of protein catabolic process; positive regulation of Wnt signaling pathway; regulation of cell cycle; regulation of chromosome separation; rhythmic process; Wnt signaling pathway ***KEGG*** Adherens junction; Circadian rhythm - plant; Measles; Ribosome biogenesis in eukaryotes; Tight junction; Wnt signaling pathway
	Tektin-3 (TEKT5)	A6H782	1.47	***GOBP*** cilium assembly; cilium movement involved in cell motility; flagellated sperm motility; regulation of brood size
	RAB2A, member RAS onco family (RAB2A)	A0A3Q1MHX8	1.43	***GOBP*** Golgi organization; macroautophagy; vesicle-mediated transport
	NADH-ubiquinone oxidoreductase 75 kDa subunit, mitochondrial (NDUFS1)	P15690	1.39	***GOBP*** mitochondrial electron transport, NADH to ubiquinone; mitochondrial respiratory chain complex I assembly ***KEGG*** Alzheimer's disease; Huntington's disease; Oxidative phosphorylation; Parkinson's disease
	NADH dehydrogenase [ubiquinone] 1 alpha subcomplex subunit 9, mitochondrial (NDUFA9)	P34943	1.38	***GOBP*** circadian rhythm; ubiquinone biosynthetic process ***KEGG*** Alzheimer's disease; Huntington's disease; Oxidative phosphorylation; Parkinson's disease
	Cytosol aminopeptidase (LAP3)	P00727	1.37	***GOBP*** Proteolysis ***KEGG*** Arginine and proline metabolism; Glutathione metabolism
	ATP synthase subunit alpha (ATP5F1A)	F1MLB8	1.35	***GOBP*** lipid metabolic process; negative regulation of endothelial cell proliferation; positive regulation of blood vessel endothelial cell migration; proton motive force-driven ATP synthesis; proton motive force-driven mitochondrial ATP synthesis
	Acetyl-coenzyme A synthetase (ACSS1)	A0A3Q1MS98	1.34	***GOBP*** acetyl-CoA biosynthetic process; acetyl-CoA biosynthetic process from acetate; lipid metabolic process
	Tektin-2 (TEKT2)	Q2T9Q6	1.31	***GOBP*** cilium assembly; cilium movement involved in cell motility; flagellated sperm motility; inner dynein arm assembly
	Izumo sperm-oocyte fusion 1 (IZUMO1)	E1BDA8	1.30	***GOBP***

(*continued on next page*)

Table 2 (*continued*)

Capacitation time	Protein name	Uniprot ID	Fold changes	Functional annotation (GO term and KEGG)
				fusion of sperm to egg plasma membrane involved in single fertilisation; heterotypic cell-cell adhesion; sperm-egg recognition
	Hydroxyacyl-coenzyme A dehydrogenase, mitochondrial	A0A3Q1LS03	1.28	***GOBP*** fatty acid beta-oxidation ***KEGG*** Lipid metabolism; fatty acid beta-oxidation.
	Coiled-coil domain containing 159 (CCDC159)	E1BD58	1.25	***GOBP***
	Septin-10 (SEPTIN10 SEPT10)	Q2KJB1	1.25	***GOBP*** cytoskeleton-dependent cytokinesis; protein localization
	Citrate synthase, mitochondrial (CS)	Q29RK1	1.24	***GOBP*** carbohydrate metabolic process; citrate metabolic process; tricarboxylic acid cycle ***KEGG*** Carbohydrate metabolism; tricarboxylic acid cycle; isocitrate from oxaloacetate
	Acyl-coenzyme A thioesterase 9, mitochondrial (ACOT9)	Q3SWX2	1.13	***GOBP*** acyl-CoA metabolic process; long-chain fatty acid metabolic process; short-chain fatty acid metabolic process ***KEGG*** Lipid metabolism; fatty acid metabolism.
	Apolipoprotein B (APOB)	E1BNR0	1.12	***GOBP*** artery morphogenesis; cellular response to lipoprotein particle stimulus; cholesterol efflux; cholesterol homeostasis; cholesterol metabolic process; cholesterol transport; establishment of localization in cell; fertilisation; flagellated sperm motility; in utero embryonic development; lipoprotein biosynthetic process; spermatogenesis triglyceride catabolic process
	Tektin-5 (TEKT5)	Q2YDI7	0.92	***GOBP*** cilium assembly; cilium movement involved in cell motility; flagellated sperm motility
	Vesicle-associated membrane protein 3 (VAMP-3)	Q2KJD2	−0.68	***GOBP*** positive regulation of receptor recycling; protein transport; retrograde transport, endosome to Golgi; SNARE complex assembly; substrate adhesion-dependent cell spreading; vesicle fusion; vesicle-mediated transport ***KEGG*** Phagosome; Salivary secretion; SNARE interactions in vesicular transport; Vasopressin-regulated water reabsorption
	A-kinase anchoring protein 3 (AKAP3)	F1MJS8	−1.05	***GOBP*** blastocyst hatching; cell surface receptor protein serine/threonine kinase signaling pathway; establishment of protein localization; flagellated sperm motility; protein localization
	Sperm mitochondria-associated cysteine-rich protein (SMCP)	Q5RZ69	−1.17	***GOBP***
	cAMP-dependent protein kinase type II-alpha regulatory subunit (PRKAR2A)	P00515	−1.27	***GOBP*** adenylate cyclase-activating G protein-coupled receptor signaling pathway ***KEGG*** Apoptosis; Insulin signaling pathway
	LOC784495 protein (LOC784495)	A1A4P8	−1.36	***GOBP***
	IQ motif containing N (IQCN)	A0A3Q1MGG8	−1.37	***GOBP***
	Zona pellucida binding protein (ZPBP)	F1N369	−1.45	***GOBP*** acrosome assembly; binding of sperm to zona pellucida
	Heat shock protein beta-9 (HSPB9)	Q2TBQ6	−1.54	***KEGG***
	Vesicle-associated membrane protein-associated protein A (VAPA)	Q0VCY1	−1.56	***GOBP*** neuron projection development; protein localization to endoplasmic reticulum
	A0A3Q1M7U3	A0A3Q1M7U3	−1.60	***GOBP*** intracellular signal transduction; regulation of signal transduction
	Actin-like protein 7A (ACTL7A)	Q32KZ2	−1.64	***GOBP*** acrosome assembly; fertilisation; single fertilisation; spermatid development
	Actin-related protein T2 (ACTRT2)	Q2TA43	−1.69	***GOBP***

Gene Ontology Biological Process (GOBP) and Kyoto Encyclopedia of Genes and Genomes (KEGG) pathways enriched among differentially expressed proteins during sperm capacitation and the acrosome reaction.

sperm capacitation and fertilisation, it also stimulates ROS production [14,25]. Therefore, we explored how the expressions of antioxidant proteins are differentially regulated during capacitation according to sperm fertility status. We used GPX4, a major intracellular antioxidant enzyme in spermatozoa [32,33], as an antioxidant marker. Similar to OXPHOS-related protein expression patterns, GPX4 protein expression was consistently expressed at higher levels during over capacitation in BNF spermatozoa than in NF spermatozoa ($p < 0.05$, Fig. 5). GPX4 was mostly detected in the head of NF spermatozoa before capacitation, whereas it was expressed in both the head and mitochondrial region of BNF spermatozoa (Fig. 5B). Similarly, abundant GPX4 protein expression was consistently detected in the sperm head and mitochondria of BNF spermatozoa until late capacitation at 120 min (Fig. 5C), consistent with our western blot results. GPX4 protein was detected in the post-equatorial region and mitochondria of NF spermatozoa following late capacitation (Fig. 5C).

3.6. Differences in the distribution of acrosomal protein and ROS during sperm capacitation according to fertility status

The levels of acrosomal vesicle-associated proteins (including ACTRT2) decreased after late capacitation (Fig. 2C). Therefore, we

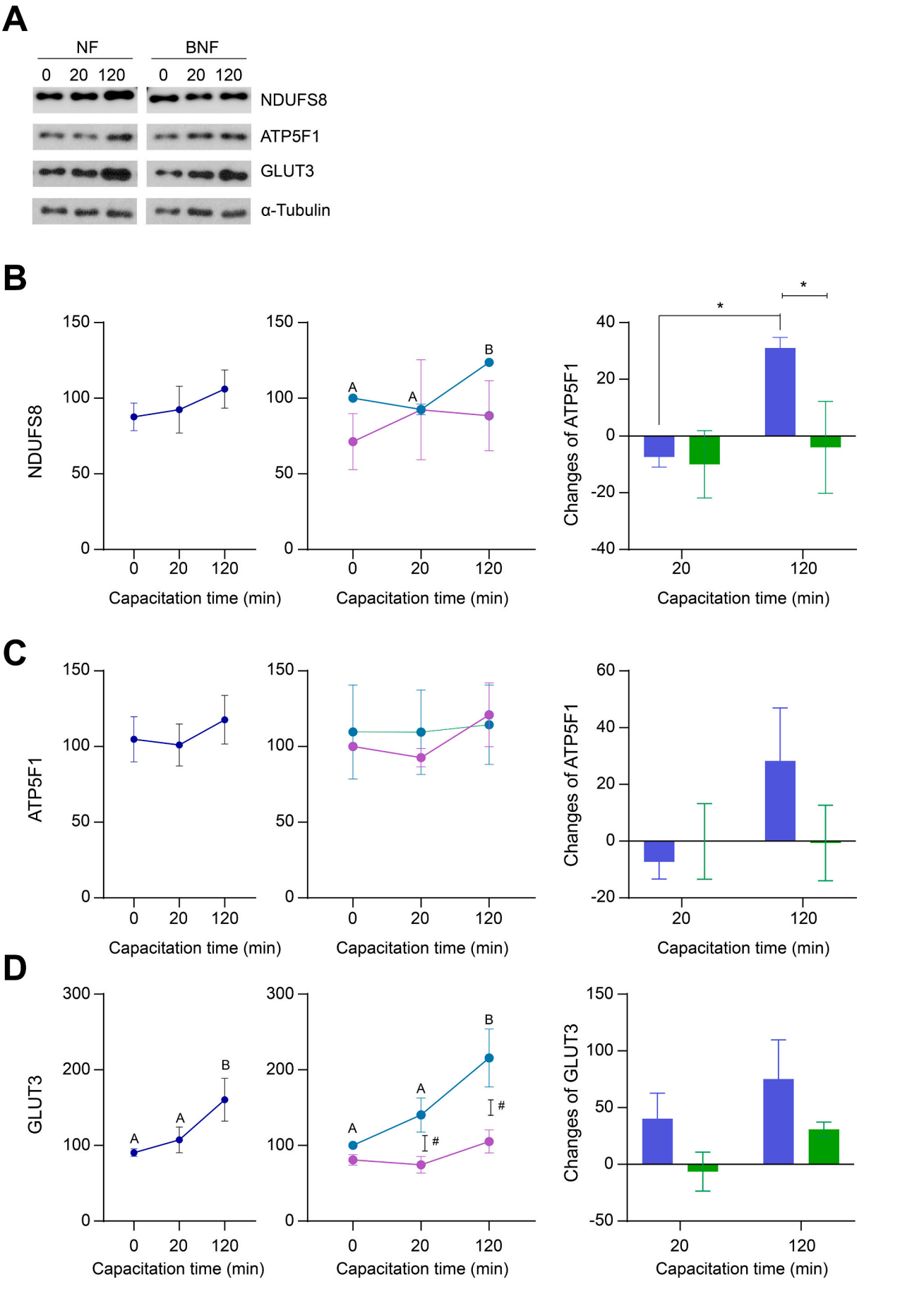

(caption on next page)

Fig. 3. Differentially expressed mitochondrial proteins during capacitation, according to sperm fertility.
(A) Representative western blot images of NDUSF8, ATP5F1, GLUT3, and α-tubulin expression. (B–D) Quantification of (B) NDUSF8, (C) ATP5F1, and (D) GLUT3 protein expression in spermatozoa regardless of fertility (left panel). Comparisons between NF (blue lines) and BNF spermatozoa (purple lines; middle panel) are shown, as are protein-expression changes following capacitation (right panel). The data shown are presented as the mean ± standard error of the mean and were analysed via two-way analysis of variance with Šídák's multiple-comparison test. A,B, significant differences in protein expression during capacitation in NF spermatozoa. a,b, significant differences in protein expression during capacitation in BNF spermatozoa. #, significant differences in protein expression between NF and BNF spermatozoa at each capacitation time.

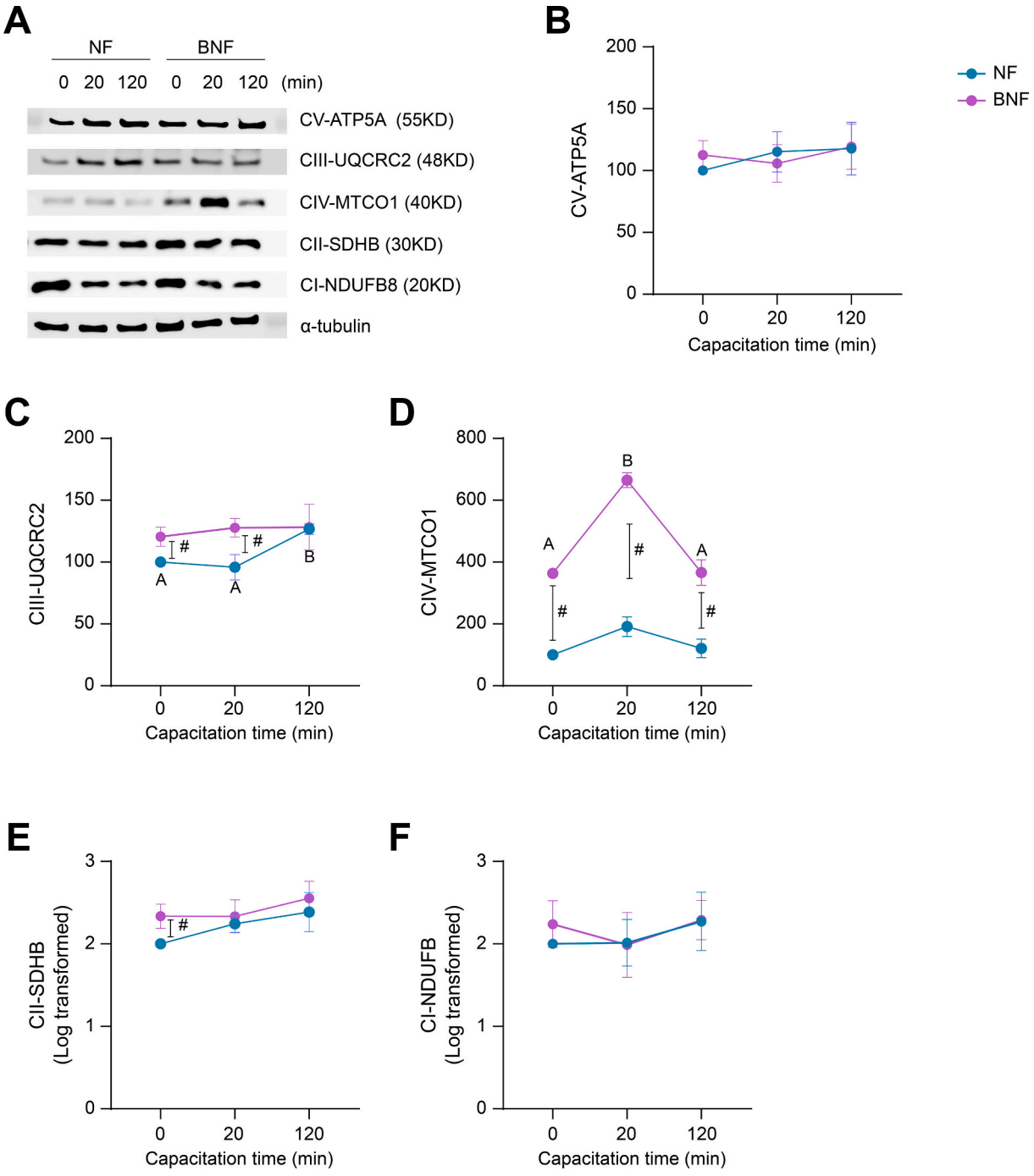

Fig. 4. Differentially expressed oxidative phosphorylation (OXPHOS)-related proteins in spermatozoa during capacitation, according to fertility.
(A) Representative western blot images of OXPHOS-related proteins in spermatozoa during capacitation. (B–F) Quantification of (B) CV-ATP5A, (C) CIII-UQCRC2, (D) CIV-MTCO1, (E) CII-SDHB, and (F) CI-NDUFB8 protein expression in NF (blue lines) and BNF (purple lines) spermatozoa. The data shown are presented as the mean ± standard error of the mean and were analysed using two-way analysis of variance with Šídák's multiple-comparison test. A,B, significant differences in protein expression during capacitation in NF spermatozoa. a,b, significant differences in protein expression during capacitation of BNF spermatozoa. #, significant differences in protein expression between NF and BNF spermatozoa at each capacitation time point.

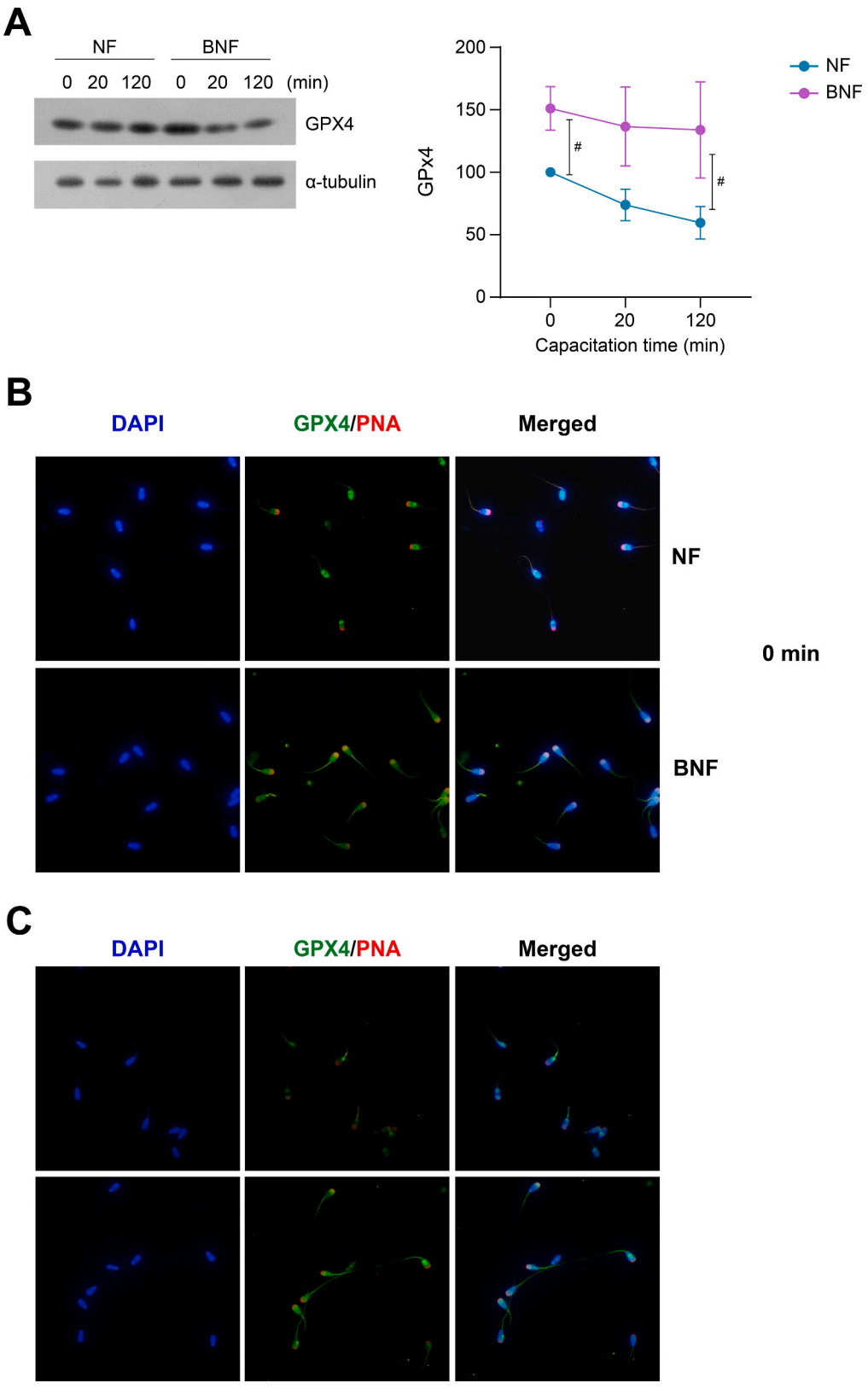

Fig. 5. Differentially GPX4 protein expression in spermatozoa during capacitation, according to fertility.
(A) Representative western blot images and quantification of GPX4 expression during capacitation between normal fertility (NF, blue line) and below-normal fertility (BNF, purple line) spermatozoa. The data shown are presented as the mean ± standard error of the mean and were analysed using two-way analysis with Šídák's multiple-comparison test. #, significant differences in protein expression between NF and BNF spermatozoa at each capacitation time. (B, C) Representative immunofluorescence images of GPX4 protein (green) and lectin peanut agglutinin PNA (acrosomal labelling, red) expression in NF and BNF spermatozoa at (B) 0 min and (C) 120 min.

determined whether ACTRT2 and acrosomal vesicle proteins were differentially expressed or localized during capacitation according to the fertility status. Spermatozoa were divided into three categories according to ACTRT2 localisation in spermatozoa, namely equatorial (post-equatorial expression), entire (smeared localisation in the entire head), and absent (no ACTRT2 protein expression).

Initially, ACTRT2 protein expression did not differ between NF and BNF spermatozoa (Fig. 6A). However, more BNF spermatozoa showed ACTRT2 protein expression in the entire sperm head following early capacitation, whereas less BNF spermatozoa showed an absence of ACTRT2 expression. No changes in ACTRT2-expression patterns were detected in NF spermatozoa during early capacitation, indicating significant differences in ACTRT2 expression between NF and BNF spermatozoa ($p < 0.01$, Fig. 6A). Importantly, smeared ACTRT2 expression in the entire sperm head increased in NF spermatozoa following late capacitation, whereas that in BNF spermatozoa decreased compared to that in early capacitation. In contrast, ACTRT2 protein expression in the equatorial sperm head decreased in NF spermatozoa, whereas it increased in BNF spermatozoa (late capacitation versus early capacitation; Fig. 6A). The abundance of spermatozoa lacking ACTRT2 expression gradually decreased in BNF spermatozoa during capacitation and diminished almost to a vanishing point after late capacitation, whereas ACTRT2 expression declined in NF spermatozoa starting from late capacitation ($p < 0.05$, Fig. 6A).

In addition, we explored the differences in acrosomal vesicle protein expression during sperm capacitation, according to fertility. Regardless of sperm fertility, over half of the spermatozoa were fully covered with acrosomal vesicle proteins, whereas the rest comprised spermatozoa with no acrosomal vesicle proteins or with degraded acrosomal vesicle proteins before capacitation (Fig. 6B). Following early capacitation, over 70 % of the spermatozoa had become degraded (51 %) or had lower acrosomal protein expression (25 %), based on comparisons with spermatozoa fully covered with acrosomal vesicle proteins. The three expression patterns of acrosomal vesicle proteins in BNF spermatozoa were comparably distributed following early capacitation and differed significantly when compared with the expression profiles in NF spermatozoa ($p < 0.01$, Fig. 6B). The percentage of NF spermatozoa with fully covered acrosomal vesicles diminished, whereas approximately half of the spermatozoa lacked acrosomal vesicle proteins or their acrosomal vesicle proteins were degraded. Although spermatozoa with degraded and diminished acrosomal vesicle proteins constituted the majority of the cell population, spermatozoa with fully covered acrosomal vesicles remained at approximately 10 % after late capacitation, resulting in significant differences between NF and BNF spermatozoa ($p < 0.01$, Fig. 6B).

To explore whether intracellular ROS levels are associated with abnormal acrosome reaction, we evaluated differences in the distribution of intracellular ROS in spermatozoa after 2 h of capacitation, based on sperm fertility status. Although most intracellular ROS signals were detected in the mitochondria of both NF and BNF spermatozoa, a small proportion of spermatozoa exhibited ROS localized in the acrosomal region. Notably, the percentage of such spermatozoa was significantly higher in the BNF group compared to the NF group ($p < 0.01$, Fig. 6C).

4. Discussion

Advanced proteomic analysis has enabled exploration of the dynamic nature of the sperm proteome during capacitation, uncovering its impact on functional changes needed to acquire fertilising ability [16,17,21,23]. In proteomics studies of proteome dynamics during capacitation, mitochondrial proteins have been most frequently highlighted, indicating that they may substantially impact capacitation [9,34]. Given the important role of mitochondria in producing ATP and ROS via OXPHOS during sperm capacitation and fertilisation, the dynamic alteration of mitochondrial proteins has been anticipated [9]. In addition to producing energy, spermatozoa undergo membrane remodelling via changes in acrosomal membrane-associated proteins, which facilitate their fusion with oocytes [16,36]. Most previous studies have focused on comparative analyses between NCP and CP spermatozoa, although some recent protein dynamics findings have revealed differences in signaling pathways in spermatozoa, depending on the capacitation status, i.e. CP versus AR spermatozoa [16,36,37]. These data indicate that a longitudinal comparative study (rather than comparative analysis based on a single time point), is required to better understand complex capacitation processes. Furthermore, considering the fertility status is necessary to achieve an in-depth understanding of how temporal changes in proteomic profiles regulate fertility. Therefore, our objective was to evaluate protein expression changes in spermatozoa during early and late capacitation and how they varied depending on the fertility status.

During capacitation and the acrosome reaction, spermatozoa undergo membrane remodelling and morphological changes, which activate acrosomal enzymes and thereby facilitate sperm–egg fusion [38]. Following the acrosome reaction, some proteins, including sperm acrosome-associated (SPACA) proteins and IZUMO1, were translocated to enhance their adhesion to oocytes [16,39,40]. Results from our previous study suggested that active synthesis and translocation of SPACA proteins during early capacitation are prerequisites for the acrosome reaction and sperm–egg fusion and, thus, fertilisation [16]. Consistent with previous findings, we observed that the expression of the IZUMO1 protein, which is essential for sperm–egg fusion [39,40], was upregulated during early capacitation. In contrast, the expression of various acrosomal vesicle proteins decreased following late capacitation. Moreover, ACTRT2 (involved in acrosomal vesicle signaling) was initially detectable in the post-equatorial region. However, punctate ACTRT2 expression was detected during early capacitation, with a gradually attenuated intensity during late capacitation. We consistently observed that strong acrosomal vesicle expression in the sperm acrosome region gradually decreased during sperm capacitation and eventually became nearly undetectable. These findings agree with previous reports showing that the release or translocation of acrosomal proteins during capacitation lowered the expression of certain proteins in AR spermatozoa [16,37]. Notably, the percentage of cells showing punctate ACTRT2 expression increased in NF spermatozoa during late capacitation, whereas it was decreased in BNF spermatozoa during late capacitation. Moreover, NF spermatozoa showed markedly accelerated acrosomal vesicle protein degradation than BNF spermatozoa during capacitation. Collectively, these results suggest that precise translocation and modification of acrosomal proteins during early capacitation are essential for ensuring the functional activity of spermatozoa, including the acrosome reaction and sperm–egg fusion, which ultimately play key roles in sperm fertility.

Sustained energy production and supply in spermatozoa is critical for them to reach their intended destination (i.e., oocytes with subsequent fertilisation). Mammalian spermatozoa rely on two spatially compartmentalized metabolic pathways—glycolysis and OXPHOS—to fulfil their energy requirements. Glycolysis, a fast-acting anaerobic process, takes place mainly in the principal piece and head of the sperm, producing two ATP molecules per glucose. In contrast, OXPHOS occurs in the midpiece, where mitochondria are concentrated, and the ATP generated is subsequently delivered to the flagellum to support motility [41]. While both metabolic systems are conserved across species, the dominant ATP-generating pathway appears to be species-dependent. Moreover, which pathway is preferentially utilized in vivo may be modulated by the microenvironment of the female reproductive tract [42]. In bull spermatozoa, OXPHOS is recognized as the principal source of ATP, particularly during capacitation, which demands substantial energy input. Notably, glucose has been shown to inhibit capacitation in bull sperm, potentially by suppressing the rise in intracellular pH necessary for this process [42]. Consistent with these observations, our proteomic analysis revealed that OXPHOS-related proteins were abundant in spermatozoa following late capacitation, regardless of the

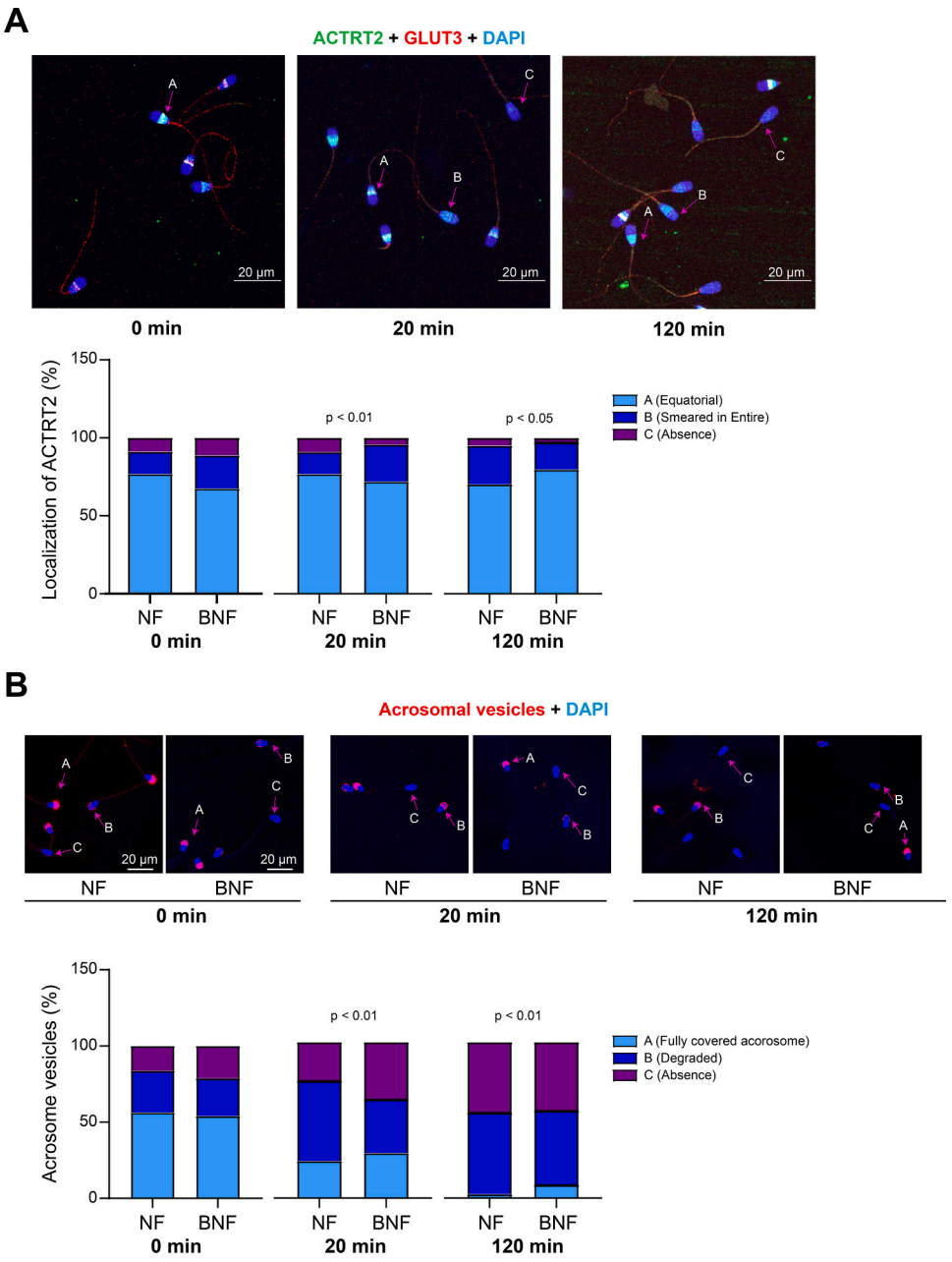

Figure 6

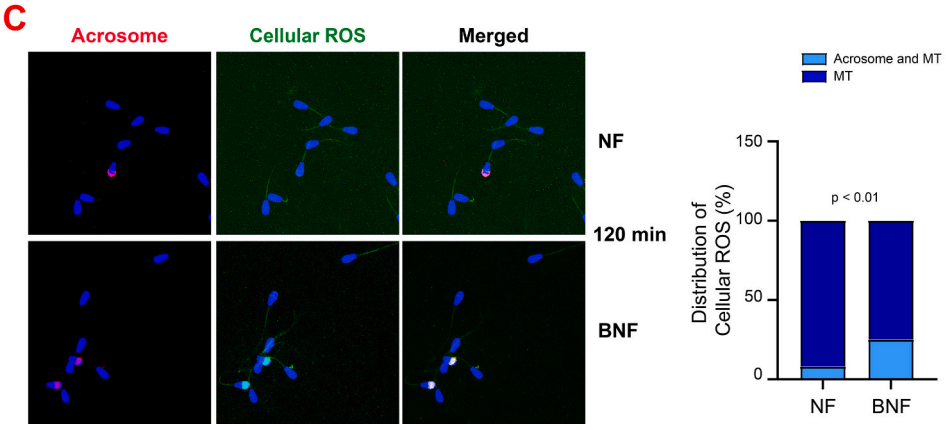

(caption on next page)

Fig. 6. Changes in actin-related protein T2 (ACTRT2) and acrosomal-vesicle protein expression in spermatozoa during capacitation, according to fertility.
(A) Representative immunofluorescence images of bovine spermatozoa after staining for ACTRT2 (green) and GLUT3 (red) following capacitation. ACTRT2 expression in spermatozoa was categorized as equatorial (A, bright green fluorescence, post-equatorial of the sperm head), smeared (B, distributed within the entire sperm head with faint green fluorescence), or absent (C, no green signal), depending on the distribution pattern observed. The percentages of NF and BNF spermatozoa in each category during capacitation (0, 20, and 120 min) are shown. The chi-square test was used to evaluate differences between NF and BNF spermatozoa. (B) Representative immunofluorescence images of bovine spermatozoa with NF and BNF after staining for acrosomal vesicle protein (red) following capacitation. Depending on the distribution pattern observed in the spermatozoa, acrosomal vesicle protein expression was categorized as a fully covered acrosome (A, bright red fluorescence within the entire acrosome region), degraded (B, some bright red fluorescence), or absent (C, no red signal). The percentages of NF and BNF spermatozoa in each category during capacitation (0, 20, and 120 min) are shown. The chi-square test was used to evaluate differences between NF and BNF spermatozoa. (C) Representative immunofluorescence images of bovine spermatozoa from NF and BNF groups after 2 h of capacitation, stained for intracellular ROS (green) and acrosomes (red). Based on fluorescence distribution, intracellular ROS localization was classified as either "acrosome + mitochondria" or "mitochondria only." The percentage of spermatozoa in each category is shown for both NF and BNF groups. Statistical differences between groups were assessed using the chi-square test.

fertility status, also indicate that the OXPHOS system is continuously activated as the main ATP supplier during bovine sperm capacitation. Notably, the expression levels of NDUFS8 and GLUT3 became elevated in NF spermatozoa following late capacitation, whereas those in BNF remained static. NDUFS8 is involved in electron transport chain complex I and participates in OXPHOS by activating electron transfer from NADH to ubiquinone, which facilitates the generation of a proton gradient and ATP production [43,44]. Importantly, we detected dynamic changes in NDUFS8 expression in NF spermatozoa during capacitation, whereas no such differences were observed in BNF spermatozoa.

No significant differences in ATP5F1 and GLUT3 protein expression occurred between NF and BNF spermatozoa during capacitation. However, the expressions of ATP5F1 and GLUT3 were continuously upregulated in BNF spermatozoa during capacitation, whereas their expression levels remained unchanged in BNF spermatozoa. These results indicate that dynamic changes in mitochondrial proteins in spermatozoa may support a steady demand for ATP during sperm capacitation and fertilisation. Complex II–IV-associated OXPHOS proteins, such as SDHB, UQCRC2, and MTCO1, were expressed at markedly higher levels in BNF spermatozoa than in NF spermatozoa before capacitation. Among them, UQCRC2 and MTCO1 showed stably higher expression levels in BNF spermatozoa than in NF spermatozoa throughout early and late capacitation. The mitochondrial complex II-associated protein, SDHB, is an enzyme located in the mitochondrial inner membrane that participates in electron transport, ROS production, and activation of the tricarboxylic acid cycle [45,46]. UQCRC2 is a subunit of complex III, a central component of the mitochondrial respiratory chain that participates in OXPHOS by transferring two electrons from ubiquinol to cytochrome *c* (Cyt c) and pumping of two protons into the intermembrane space [47]. Cyt c, as an electron carrier, transfers four electrons to accelerate the O_2 reduction to H_2O in complex IV, which contains the MTCO1 subunit [48]. Simultaneously, complex IV contributes to the proton gradient required for ATP production by actively pumping protons into the intermembrane space [49]. Therefore, to maintain appropriate cellular ROS levels, complex III reduces O_2 to produce superoxide via ubiquinone (which transfers a single electron to O_2), whereas complex IV transfers an electron to reduce O_2 to H_2O [50,51]. MT-CO1 overexpression can increase apoptosis- and DNA damage-associated genes via excessive ROS production, which in turn leads to epigenetic alterations that accelerate the metabolic features of the pro-cancerous phenotype [52]. Moreover, high ROS levels were detected in mice with age-related MT-CO1 mutations, which shortened the lifespan [53]. Since ROS are primarily generated as by-products of cellular respiration [54], we hypothesized that excessive OXPHOS activity in spermatozoa may result in abnormal respiration and elevated ROS production, potentially compromising their fertility outcomes. Moreover, as excessive ROS has been reported to negatively affect the acrosome reaction, whereas low levels of ROS play a crucial regulatory role in this process [55], our data support this concept by demonstrating that intracellular ROS in the acrosome were more abundant in BNF spermatozoa than in NF spermatozoa. These findings support our hypothesis that abnormal and elevated intracellular ROS in the acrosomal region may delay the acrosome reaction, ultimately leading to reduced male fertility. These results, along with previous evidence [16,56,57], imply that the molecular impairments detected in BNF spermatozoa may play a critical role in subfertility. Moreover, the GPX4 protein, a major mitochondrial antioxidant enzyme [32], was continuously maintained at higher levels in BNF spermatozoa than in NF spermatozoa during capacitation, suggesting that the antioxidant system was activated to reduce the oxidative stress-derived imbalances in complexes III and IV in BNF spermatozoa during capacitation. We designed our experiment to examine two pivotal capacitation points—early and late capacitation stages in order to identify differences in the stage-specific changes according to fertility. Importantly, sperm motility and motion kinematics showed only minimal changes during the early capacitation, while tyrosine phosphorylation and redistribution of acrosomal vesicle proteins were evident at this stage, suggesting that molecular changes required to maintain fertilising capacity begin early, even in the absence of substantial motility changes. In contrast, the late phase of capacitation was characterized by a significant increase in sperm velocity parameters (VAP and VSL) and linearity, which coincided with the upregulation of OXPHOS-related proteins. These findings indicate that while early capacitation involves key molecular (especially acrosomal vesicles) rearrangements supporting fertilisation potential, late capacitation promotes enhanced motility through mitochondrial activation. Therefore, this dual-time and different fertility status approach enabled the identification of temporal molecular alterations associated with progressive capacitation and the acrosome reaction, and allowed us to correlate protein expression profiles with distinct functional sperm states. Notably, OXPHOS-related and acrosome vesicle proteins exhibited clear stage- and fertility-dependent expression patterns, highlighting their potential as time-sensitive biomarkers of capacitation and sperm fertility.

In this study, we used heparin as the capacitation inducer based on its well-established efficacy in bovine sperm and physiological relevance to in vivo conditions, particularly the presence of heparin-like glycosaminoglycans in the female reproductive tract [61–63]. This concentration was previously optimized in our laboratory to induce capacitation effectively without compromising sperm viability, and has also been applied in sperm penetration assays to predict fertility with over 95 % accuracy [24]. The use of a standardized inducer ensured comparability of proteomic profiles across samples. Nevertheless, further studies using alternative inducers such as calcium may provide additional insights into the diverse molecular mechanisms underlying capacitation and fertility. As a preliminary study, we evaluated heparin-treated sperm at 0, 20, 30, 60, 120, and 240 min. Capacitation markers significantly increased by 20 min, while the highest proportion of acrosome-reacted spermatozoa was observed at 120 min. Incubation beyond 4 h markedly reduced sperm viability (<50 %) and motility (<25 %). Based on these findings, we defined 20 min as the early and 120 min as the late capacitation stages, as they represent biologically relevant time points without excessive cell damage. Several studies have reported that cryopreservation can induce premature or capacitation-

like changes, contributing to reduced sperm longevity in the female reproductive tract [58,59]. Capacitation in frozen-thawed spermatozoa using inducers like heparin typically occurs within 15 min to 1 h [59,64]. However, we acknowledge a limitation of this study: capacitation-associated changes may vary between fresh and frozen-thawed spermatozoa, and given that in vivo capacitation of fresh spermatozoa may require extended incubation (>4 h), our selected time points may not comprehensively reflect the full temporal dynamics in fresh samples [60]. Thus, future studies with extended time points in fresh semen samples are necessary to further elucidate how capacitation timing affects sperm fertility in the female reproductive tract.

5. Conclusion

We detected a systemic crisis, including (1) aberrant translocation and delayed acrosome reaction and (2) hyper-activation of the mitochondrial respiratory system, involving complex III and IV, during sperm capacitation in BNF spermatozoa. Moreover, we found that BNF spermatozoa exhibit a delayed acrosome reaction during capacitation, which is associated with the accumulation of intracellular ROS in the acrosomal region until late capacitation. In addition, GPX4 protein remained highly expressed in BNF spermatozoa throughout capacitation, suggesting a potential ROS-associated risk factor for reduced sperm fertility. Based on our results, we suggest that sperm fertility is maintained by multiple interrelated factors, including the spatiotemporal translocation of acrosomal proteins during capacitation and the appropriate activation of mitochondrial proteins. To substantiate these findings, further studies are required to elucidate how temporal intracellular ROS levels and the OXPHOS system change during sperm capacitation according to the fertility status. We believe that the results of this study might help uncover the spatiotemporal regulatory system of sperm fertility as sperm migrate through the female reproductive tract and support the development of therapeutic methods for male infertility and contraceptive targets to regulate the acrosome reaction and mitochondrial activity of spermatozoa.

Supplementary data to this article can be found online at https://doi.org/10.1016/j.ijbiomac.2025.146349.

Glossary

ACTRT2	actin-related protein T2
AR	acrosome-reacted
ATP	adenosine triphosphate
ATP5F1	ATP synthase F (0) complex subunit B1, mitochondrial
BNF	below-normal fertility
CP	capacitated
CTC/H33258	chlortetracycline/Hoechst
Cyt c	cytochrome *c*
GLUT3	glucose transporter 3
GPX4	glutathione peroxidase 4
IZUMO1	Izumo sperm–egg fusion protein 1
MTCO1	cytochrome *c* oxidase subunit I
NCP	non-capacitated
NDUFS8	NADH: ubiquinone oxidoreductase core subunit S8
NF	normal fertility
SDHB	succinate dehydrogenase complex iron sulphur subunit B
SPACA	sperm acrosome-associated
TFA	trifluoroacetyl acid
UQCRC2	ubiquitin-cytochrome *c* reductase core protein 2

CRediT authorship contribution statement

Yoo-Jin Park: Writing – review & editing, Writing – original draft, Investigation, Funding acquisition, Formal analysis, Conceptualization. **Gangaraju Gedda:** Writing – review & editing, Investigation, Data curation. **Myung-Geol Pang:** Writing – review & editing, Writing – original draft, Resources, Methodology, Funding acquisition, Conceptualization.

Funding

This work was supported by the Basic Science Research Program through the National Research Foundation of Korea [grant numbers RS-2024-00343755, NRF-2018R1A6A1A03025159], funded by the Ministry of Education.

Declaration of competing interest

The authors have nothing to declare.

Acknowledgements

We thank the BT Research Facility Center at Chung-Ang University for assistance. We thank the Korea Basic Science Institute (Ochang Headquarters, Division of Bioconvergence Analysis) for performing the nano LC-LTQ-Orbitrap analysis.

Data availability

Data will be made available on request.

References

[1] World Health Organization, Infertility, Available from: https://www.who.int/news-room/fact-sheets/detail/infertility, 2024.
[2] M. Macaluso, et al., A public health focus on infertility prevention, detection, and management, Fertil. Steril. 93 (1) (2010), p. 16 e1-10.
[3] Y.J. Hwang, et al., Psychiatric considerations of infertility, Psychiatry Investig. 21 (11) (2024) 1175–1182.
[4] S.A. Carson, A.N. Kallen, Diagnosis and management of infertility: a review, JAMA 326 (1) (2021) 65–76.
[5] N.M. van den Boogaard, et al., Improving the implementation of tailored expectant management in subfertile couples: protocol for a cluster randomized trial, Implement. Sci. 8 (2013) 53.
[6] F.A. Kersten, et al., Overtreatment in couples with unexplained infertility, Hum. Reprod. 30 (1) (2015) 71–80.
[7] H. Sun, et al., Global, regional, and national prevalence and disability-adjusted life-years for infertility in 195 countries and territories, 1990-2017: results from a global burden of disease study, 2017, Aging (Albany NY) 11 (23) (2019) 10952–10991.
[8] Y. Zhou, et al., The role of alginate oligosaccharide on boar semen quality: a research review, Int. J. Biol. Macromol. 277 (Pt 3) (2024) 134492.
[9] B.M. Lee, et al., Boar fertility is controlled through systematic changes of mitochondrial protein expression during sperm capacitation, Int. J. Biol. Macromol. 248 (2023) 125955.
[10] Y.J. Park, W.K. Pang, M.G. Pang, Integration of omics studies indicates that species-dependent molecular mechanisms govern male fertility, J. Anim. Sci. Biotechnol. 14 (1) (2023) 28.
[11] A. Khatun, M.S. Rahman, M.G. Pang, Clinical assessment of the male fertility, Obstet. Gynecol. Sci. 61 (2) (2018) 179–191.
[12] Y. Chen, et al., Identification of new protein biomarkers associated with the boar fertility using iTRAQ-based quantitative proteomic analysis, Int. J. Biol. Macromol. 162 (2020) 50–59.
[13] J. Ribas-Maynou, et al., Determination of double- and single-stranded DNA breaks in bovine sperm is predictive of their fertilizing capacity, J. Anim. Sci. Biotechnol. 13 (1) (2022) 105.
[14] Y.J. Park, M.G. Pang, Mitochondrial functionality in male fertility: from spermatogenesis to fertilization, Antioxidants (Basel) 10 (1) (2021) 98.
[15] Y.J. Park, et al., Low sperm motility is determined by abnormal protein modification during epididymal maturation, World J. Mens Health 40 (3) (2022) 526–535.
[16] Y.J. Park, et al., Spatiotemporal translation of sperm acrosome associated proteins during early capacitation modulates sperm fertilizing ability, J. Adv. Res. (2025), https://doi.org/10.1016/j.jare.2025.03.035. Online ahead of print.
[17] W. Yang, et al., High-resolution LC-MS/MS combined with TMT quantitative proteomic analysis reveals regulatory mechanism of sperm capacitation by heparin, Ca(2+) and BSA, Int. J. Biol. Macromol. 305 (Pt 2) (2025) 141349.
[18] C. Diez-Sanchez, et al., Mitochondria from ejaculated human spermatozoa do not synthesize proteins, FEBS Lett. 553 (1–2) (2003) 205–208.
[19] B.M. Gadella, et al., Sperm head membrane reorganisation during capacitation, Int. J. Dev. Biol. 52 (5–6) (2008) 473–480.
[20] P.E. Visconti, Understanding the molecular basis of sperm capacitation through kinase design, Proc. Natl. Acad. Sci. USA 106 (3) (2009) 667–668.

[21] W.S. Kwon, et al., A comprehensive proteomic approach to identifying capacitation related proteins in boar spermatozoa, BMC Genomics 15 (1) (2014) 897.
[22] G. Su, et al., Spirulina polysaccharides improve postthaw sperm quality in bulls by inhibiting the activation of pathways related to protein kinase A, Int. J. Biol. Macromol. 296 (2025) 139796.
[23] C. Mahe, et al., The sperm-interacting proteome in the bovine isthmus and ampulla during the periovulatory period, J. Anim. Sci. Biotechnol. 14 (1) (2023) 30.
[24] Y.J. Park, et al., Sperm penetration assay as an indicator of bull fertility, J. Reprod. Dev. 58 (4) (2012) 461–466.
[25] Z. Zhu, et al., Negative effects of ROS generated during linear sperm motility on gene expression and ATP generation in boar sperm mitochondria, Free Radic. Biol. Med. 141 (2019) 159–171.
[26] Y.J. Park, et al., Fertility-related proteomic profiling bull spermatozoa separated by percoll, J. Proteome Res. 11 (8) (2012) 4162–4168.
[28] W.K. Pang, et al., Heat shock protein family D member 1 in boar spermatozoa is strongly related to the litter size of inseminated sows, J. Anim. Sci. Biotechnol. 13 (1) (2022) 42.
[29] S. Tyanova, et al., The Perseus computational platform for comprehensive analysis of (prote)omics data, Nat. Methods 13 (9) (2016) 731–740.
[30] J.D. Rudolph, J. Cox, A network module for the Perseus software for computational proteomics facilitates proteome interaction graph analysis, J. Proteome Res. 18 (5) (2019) 2052–2064.
[31] D.Y. Ryu, et al., Capacitation and acrosome reaction differences of bovine, mouse and porcine spermatozoa in responsiveness to estrogenic compounds, J. Anim. Sci. Technol. 56 (2014) 26.
[32] H. Imai, et al., Depletion of selenoprotein GPx4 in spermatocytes causes male infertility in mice, J. Biol. Chem. 284 (47) (2009) 32522–32532.
[33] B. Ozkosem, et al., Advancing age increases sperm chromatin damage and impairs fertility in peroxiredoxin 6 null mice, Redox Biol. 5 (2015) 15–23.
[34] M. Castello-Ruiz, et al., Effect of capacitation on proteomic profile and mitochondrial parameters of spermatozoa in bulls, J. Proteome Res. 24 (4) (2025) 1817–1831.
[36] N. Chhikara, et al., Proteomic changes in human spermatozoa during in vitro capacitation and acrosome reaction in normozoospermia and asthenozoospermia, Andrology 11 (1) (2023) 73–85.
[37] J. Castillo, et al., Proteomic changes in human sperm during sequential in vitro capacitation and acrosome reaction, Front. Cell Dev. Biol. 7 (2019) 295.
[38] M. Okabe, The cell biology of mammalian fertilization, Development 140 (22) (2013) 4471–4479.
[39] T. Noda, et al., Sperm proteins SOF1, TMEM95, and SPACA6 are required for sperm-oocyte fusion in mice, Proc. Natl. Acad. Sci. USA 117 (21) (2020) 11493–11502.
[40] N. Inoue, et al., Oocyte-triggered dimerization of sperm IZUMO1 promotes sperm-egg fusion in mice, Nat. Commun. 6 (2015) 8858.
[41] P.E. Visconti, Sperm bioenergetics in a nutshell, Biol. Reprod. 87 (3) (2012) 72.
[42] B.T. Storey, Mammalian sperm metabolism: oxygen and sugar, friend and foe, Int. J. Dev. Biol. 52 (5–6) (2008) 427–437.
[43] V. Procaccio, et al., cDNA sequence and chromosomal localization of the NDUFS8 human gene coding for the 23 kDa subunit of the mitochondrial complex I, Biochim. Biophys. Acta 1351 (1–2) (1997) 37–41.
[44] Q.W. Xiong, et al., The requirement of the mitochondrial protein NDUFS8 for angiogenesis, Cell Death Dis. 15 (4) (2024) 253.
[45] B.A. Ackrell, Cytopathies involving mitochondrial complex II, Mol. Asp. Med. 23 (5) (2002) 369–384.
[46] C.L. Quinlan, et al., Mitochondrial complex II can generate reactive oxygen species at high rates in both the forward and reverse reactions, J. Biol. Chem. 287 (32) (2012) 27255–27264.
[47] G. Lenaz, et al., The role of Coenzyme Q in mitochondrial electron transport, Mitochondrion 7 (Suppl) (2007) S8–33.
[48] M. Brischigliaro, et al., Mitochondrial cytochrome c oxidase defects alter cellular homeostasis of transition metals, Front. Cell Dev. Biol. 10 (2022) 892069.
[49] M.M. Pereira, M. Santana, M. Teixeira, A novel scenario for the evolution of haem-copper oxygen reductases, Biochim. Biophys. Acta 1505 (2–3) (2001) 185–208.
[50] R. Guo, et al., Architecture of human mitochondrial respiratory megacomplex I(2)III(2)IV(2), Cell 170 (6) (2017) 1247–1257 e12.
[51] E. Lapuente-Brun, et al., Supercomplex assembly determines electron flux in the mitochondrial electron transport chain, Science 340 (6140) (2013) 1567–1570.
[52] R.K. Singh, et al., Role of ectopically expressed mtDNA encoded cytochrome c oxidase subunit I (MT-COI) in tumorigenesis, Mitochondrion 49 (2019) 56–65.
[53] G. Reichart, et al., Mitochondrial complex IV mutation increases reactive oxygen species production and reduces lifespan in aged mice, Acta Physiol (Oxford) 225 (4) (2019) e13214.
[54] Y. Mateo-Otero, et al., Sperm physiology and in vitro fertilising ability rely on basal metabolic activity: insights from the pig model, Commun. Biol. 6 (1) (2023) 344.
[55] T. Ichikawa, et al., Reactive oxygen species influence the acrosome reaction but not acrosin activity in human spermatozoa, Int. J. Androl. 22 (1) (1999) 37–42.
[56] D.Y. Liu, H.W. Baker, Disordered acrosome reaction of spermatozoa bound to the zona pellucida: a newly discovered sperm defect causing infertility with reduced sperm-zona pellucida penetration and reduced fertilization in vitro, Hum. Reprod. 9 (9) (1994) 1694–1700.
[57] K. Li, et al., Inhibition of sperm capacitation and fertilizing capacity by adjudin is mediated by chloride and its channels in humans, Hum. Reprod. 28 (1) (2013) 47–59.
[58] J.L. Bailey, J.F. Bilodeau, N. Cormier, Semen cryopreservation in domestic animals: a damaging and capacitating phenomenon, J. Androl. 21 (1) (2000) 1–7.
[59] R. Zhang, et al., Heparin-induced and caffeine or ouabain supplemented capacitation of frozen-thawed yak (Bos grunniens) spermatozoa, Reprod. Domest. Anim. 57 (6) (2022) 587–597.
[60] J.J. Parrish, et al., Capacitation of bovine sperm by heparin, Biol. Reprod. 38 (5) (1988) 1171–1180.
[61] R.R. Handrow, N.L. First, J.J. Parrish, Calcium requirement and increased association with bovine sperm during capacitation by heparin, J. Exp. Zool. 252 (2) (1989) 174–182.
[62] H.L. Galantino-Homer, P.E. Visconti, G.S. Kopf, Regulation of protein tyrosine phosphorylation during bovine sperm capacitation by a cyclic adenosine 3′5’-monophosphate-dependent pathway, Biol. Reprod. 56 (3) (1997) 707–719.
[63] H.L. Galantino-Homer, et al., Bovine sperm capacitation: assessment of phosphodiesterase activity and intracellular alkalinization on capacitation-associated protein tyrosine phosphorylation, Mol. Reprod. Dev. 67 (4) (2004) 487–500.
[64] G. Kadirvel, et al., Capacitation status of fresh and frozen-thawed buffalo spermatozoa in relation to cholesterol level, membrane fluidity and intracellular calcium, Anim. Reprod. Sci. 116 (3–4) (2009) 244–253.